

Effect of silver-doping on the structural, topography and optical CdSe thin films

R. I. Jasim^a, E. H. Hadi^a, S. S. Chiad^a, N. F. Habubi^b, M. Jadan^{c,d}, J. S. Addasi^{e,*}

^a*Department of Physics, College of Education, Mustansiriyah University, Baghdad, Iraq*

^b*Department of Engineering of Refrigeration and Air Conditioning Technologies, Alnukhba University College, Baghdad, Iraq*

^c*Department of Physics, College of Science, Imam Abdulrahman Bin Faisal University, P.O. Box 1982, 31441 Dammam, Saudi Arabia*

^d*Basic and Applied Scientific Research Center, Imam Abdulrahman Bin Faisal University, P.O. Box 1982, 31441 Dammam, Saudi Arabia*

^e*Department of Applied Physics, College of Science, Tafila Technical University, P.O. Box 179, 66110 Tafila, Jordan*

Using thermal evaporation, thin films of silver-doped CdSe were synthesized on glass bases. A hexagonal structure with a preference orientation along (100) plane according to the X-ray diffraction pattern. The surface topography was determined using Atomic Force Microscopy (AFM). AFM detects spherical nature nanoparticles and roughness rate of the CdSe thin film decreases and the root mean square decreases with (2 and 4) % doping in silver. As the doping content increase, the optical energy bandgap decrease from 1.85 eV to 1.75 eV. Optical analysis indicates that Ag doping in CdSe results in a redshift in band edge.

(Received December 11, 2022; Accepted March 9, 2023)

Keywords: CdSe, Ag, Thermal evaporation technique, XRD, AFM, Optical properties

1. Introduction

In the past decade, CdSe, has acquired quite heed for its special optical properties and electrical characterization [1, 2]. In addition to its optical properties, CdSe is a significant semiconductor material because its small direct band gap (~1.71 eV) in zinc blende structure phase and ~1.8 eV in the wurtzite crystal phase [3]. Cadmium selenide is a combination of Cadmium (Cd) from group 2 and Selenium (Se) from group 6. It is an n-type semiconductor. thin films of CdSe can be utilized for photovoltaic applications because of a suitable direct band gap for bulk CdSe material, good electrical conductivity, and high absorption [4–6]. As a result of the ionic produced by Cd⁺² and Se⁻² ions exceeding that of CdSe, CdSe is formed into thin films. Cd⁺² and Se⁻² ions control the film formation [7]. As nanocrystalline size decreases, the energy gap increases due to the effect of spacing between energy levels [8, 9]. Because of the large surface to volume ratio of very small particles the surface effects become significant for clusters containing few atoms. There have been very few studies on the effect of doping on CdSe via thermal evaporation at room temperature on glass substrates. Incorporating impurity atoms into crystal lattices to modify physical properties through impurity levels by using In, Sb, Ag, and Zn [10, 11]. A variety of growth methods were employed to deposit CdSe thin films comprising, PLD [12], thermal evaporation [13, 14], CBD [15], spray pyrolysis [16] and electrodeposition [17]. In this article, the investigation of band gap, absorption, refractive index and extinction coefficient and transmittance spectra of CdSe and CdSe:Ag films by thermal evaporation method were studied.

* Corresponding author: addasijihad@gmail.com
<https://doi.org/10.15251/JOR.2023.192.187>

2. Experimental

CdSe thin films with silver doped were prepared using a thermal co-evaporation technique, by using a vacuum coating unit 2×10^{-5} torr is achieved. In a molybdenum boat, Cadmium Selenide powder must be taken in a specific weight, take 2 % and 4 % from this weight Silver and put it in other molybdenum boat. The base was chemically and ultrasonically cleaned. At a distance of roughly 10 cm, this slide was placed above (CdSe and Ag). The films thickness in the range of (1 μ m) was determined by interference method and the rate of deposition was 50 nm/min. The structural characterizations were analyzed by XRD. AFM was employed to study film surface. The optical transmittance and absorbance were detected using UV-Visible spectrophotometer.

3. Results and discussions

3.1. Structural studies

Scans 2θ between 20° and 60° was performed on pure and Ag-doped CdSe. For pure CdSe, the peaks are detected at $2\theta = 23.82^\circ$, 45.79° and 63.82° attributed to the (100), (203) and (202) planes respectively, whereas in silver (2 and 4 %) doped films. XRD patterns suggest that the studied films are polycrystalline and have a hexagonal (wurtzite) structure. Therefore, the peak position on doping has shifted. The CdSe phase shows three dominant peaks at 23.82° , 45.79° and 63.82° attributed to the (100), (203) and (202) planes respectively [18]. The crystallite size computes for preferential orientation along (100) plane standard JCPDS card No (00-019-019). The strongest diffraction peak corresponds to the (100) plane. With an increase in doping concentration, the crystallinity of the film increases slightly. As a result of the large number of dopants occupying the interstitial spaces in the crystal lattice of CdSe, the crystalline character increases. The angle of diffraction shifts slightly after doping, Consequently, the increased interplanar distance is the result of replacing smaller Cd ionic radii (0.097 nm) with larger Ag ionic radii (0.126 nm). As measured on the (100) diffraction plane, CdSe: Ag has a slightly smaller full width at half maxima than undoped CdSe [19]. The Scherrer formula is utilized to obtain crystallite size (D) for preferred planes [hkl] for thermally evaporated CdSe thin films [20, 21]:

$$D = \frac{k\lambda}{\beta \cos\theta} \quad (1)$$

where $k = 0.94$, where θ is Bragg's angle, λ is the wavelength of X-rays, β is FWHM. The corresponding D increases from 12.69 nm (CdSe) to 14 nm and 15 nm (CdSe:Ag (2 and 4) %), this may be due to differences in ionic radii between Cd and silver [22].

The microstrain value (ϵ) was evaluated and the density of dislocation (δ) has been calculated by via equation (2) and (3) as the following [23, 24]:

$$\epsilon = \frac{\beta \cos\theta}{4} \quad (2)$$

$$\delta = \frac{1}{D^2} \quad (3)$$

The micro-strain and dislocation density decrease with an increase in Ag content. This parameter is also influenced by D because as D increases, the crystallite boundaries as imperfections in crystal structure are reduced [25]. The crystal lattice can expand due to the larger radius of the dopant atoms [5]. Table 1 shows the structure parameter of all films.

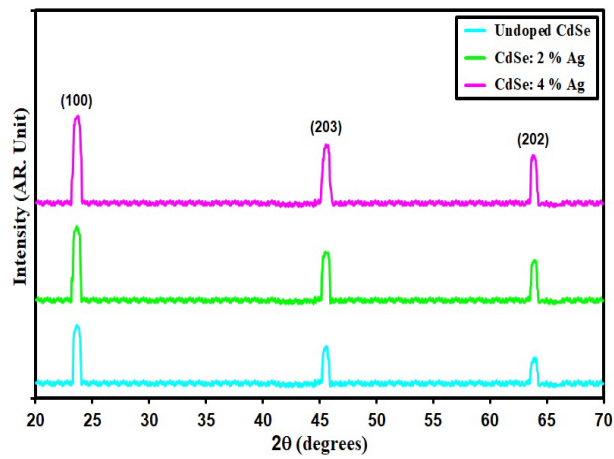


Fig. 1. XRD styles of the intended films.

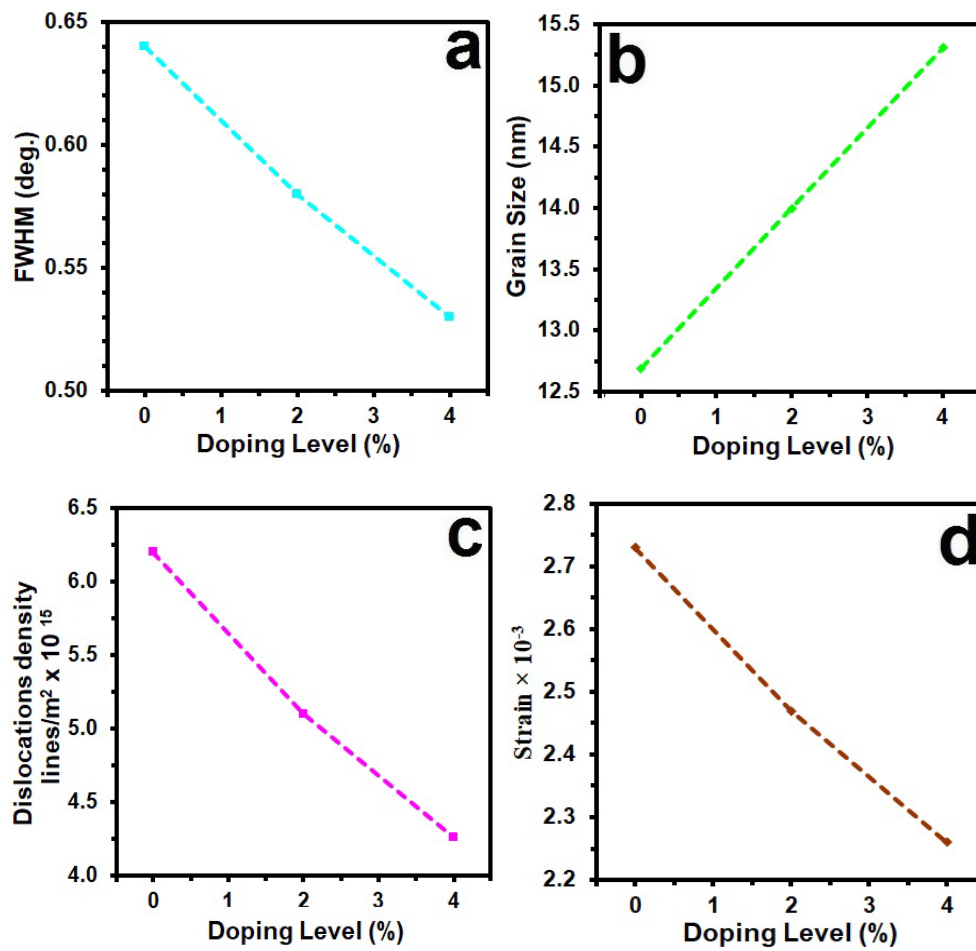


Fig. 2. X-ray parameters of pure & Ag doped CdSe films.

Table 1. Structure parameters of intended films.

Specimen	2θ ($^{\circ}$)	(hkl) Plane	FWHM ($^{\circ}$)	Optical bandgap (eV)	Grain size (nm)	Dislocations density ($\times 10^{15}$) (lines/m 2)	Strain ($\times 10^{-3}$)
Undoped CdSe	23.83	100	0.64	1.85	12.69	6.20	2.73
CdSe: 2% Ag	23.79	100	0.58	1.80	14.00	5.10	2.47
CdSe: 4% Ag	23.76	100	0.53	1.75	15.31	4.26	2.26

3.2. Surface topography study

According to the AFM results shown in figure (3), By increasing dopant percentage, grain size decreases, which is concurred with XRD measurements. Furthermore, Comparing, Scherrer's equation (2) and AFM measurements, we can observe a difference in particle size values. Increasing in grain size indicated good crystallization, which improves the performance of a device [26]. As shown in Table 2, the root mean square of the surface roughness decreased with the increased doping proving that the grains were uniformly distributed with all surface area. The roughness rate of the CdSe thin film decreased from 7.74 nm to 3.69 nm and the root mean square decrease from 9.36 nm to 5.26 nm with 4% doping in silver. It was obvious that the surface was smooth with a decrease of the root mean square in CdSe:Ag thin film led to the increasing crystalline. Also, the increase of the grain size by increasing to the surface homogeneity, and this result agreed with XRD results.

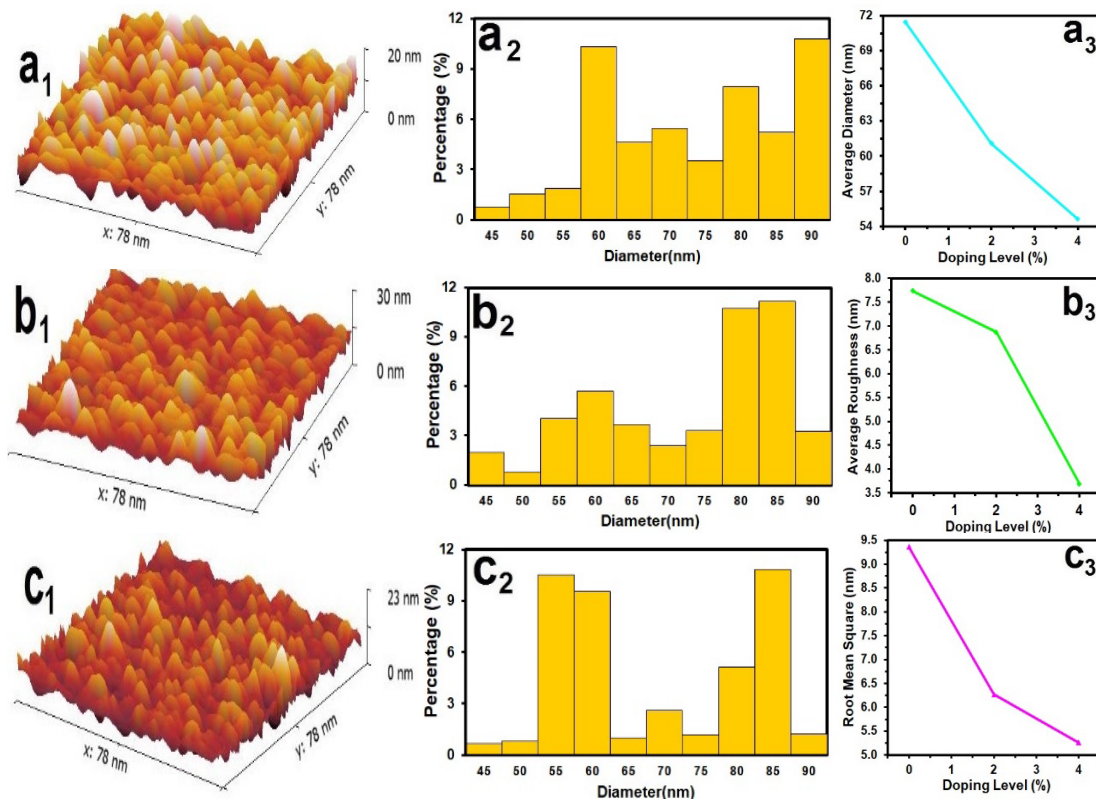


Fig. 3. AFM of pure and CdSe:Ag films.

Table 2. AFM parameter measurement of pure & CdSe:Ag films.

Samples	Average Particle size (nm)	R _a (nm)	R. M. S. (nm)
Undoped CdSe	71.42	7.74	9.36
CdSe: 2 % Ag	61.08	6.87	6.27
CdSe: 4 % Ag	54.63	3.69	5.26

3.3. Optical properties study

Spectra of the transmittance (T) of the grown films were measured in ranging of wavelengths 300-900 nm to understand their optical properties as shown in figure 4, Variations in transmission via wavelength of CdSe and CdSe: (2 and 4) % silver films. The shifts of transmittance spectrum to shorter wavelengths with increasing of silver for all samples. It can have noticed that the transmission decreases after doped CdSe films with silver due to the effect of impurities atoms, which is working on the composition of localized states in band gap [27, 28].

By using the following equation, the sample absorption coefficient (α), was determined [29, 30]:

$$\alpha = \frac{1}{d} \ln \frac{1}{T} \quad (4)$$

where d is film thickness. As shown in figure 5, α varies with photon energy. Also, With increasing doping concentration, the absorption coefficient increases. It was found that Ag acts as trap centers and increases α . In the case of silver doped samples, a different absorption mechanism is possible. CdSe thin films with silver-doping show an increase in charge carrier concentration in the conduction band because of Ag content. As a result of this electron-photon interaction, additional electrons can be incorporated in the process of absorption of incident photons, which ultimately increases the absorption coefficient [31]. The samples all exhibit high absorption in the visible region, making them promising candidates for use in thin film solar cells.

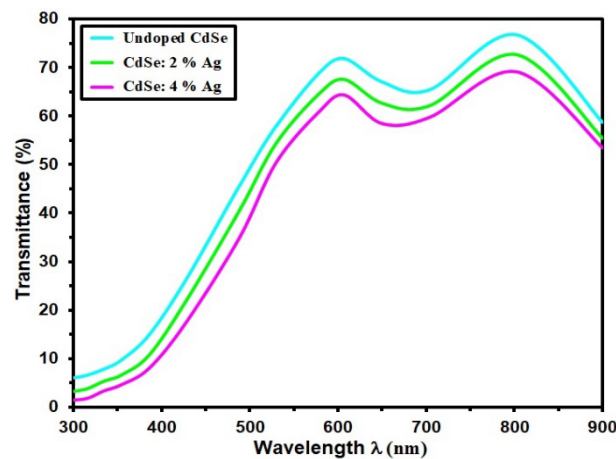


Fig.4. Transmittance of pure & CdSe:Ag films with different dopants.

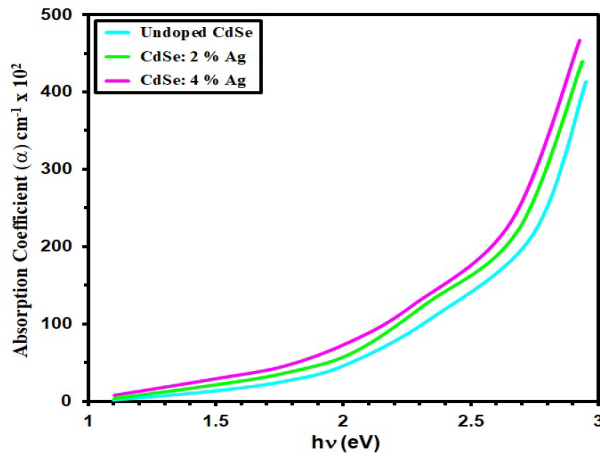


Fig. 5. α of pure & CdSe:Ag films with different dopants.

The equation below was used to determine the optical energy band gap E_g of the undoped and Ag-doped CdSe thin films [32, 33]:

$$\alpha h\nu = B(h\nu - E_g)^{\frac{1}{2}} \tag{5}$$

B represents a constant. The variation of $(\alpha h\nu)^2$ can be shown as a function of $h\nu$. As shown in Figure 6. In figure 6 and Table 3. It is noticed when silver doping is increased, E_g decreases from 1.85 eV to 1.75 eV. Due to trap tailing levels in band gap, the optical band gap is decreasing along with localized states in this region. [34, 35]. CdSe thin films can be improved by silver doping based on the decreasing of the optical energy gap.

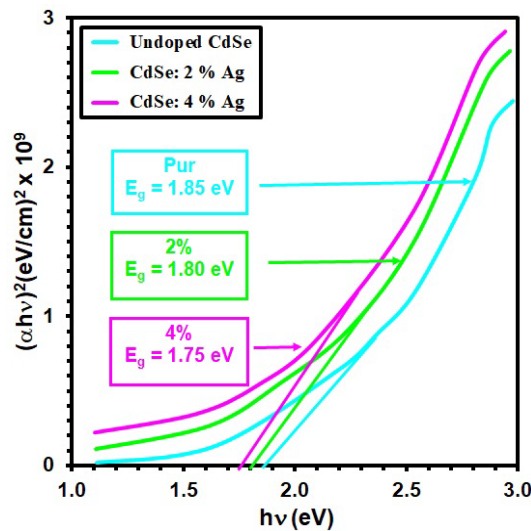


Fig. 6. Direct band gap (E_g) of pure & CdSe:Ag films with different dopants.

The extinction coefficient (k) was calculated using Eq. (6) [36, 37]:

$$K = \frac{\alpha\lambda}{4\pi} \tag{6}$$

Figure (7) shows that the decrease in value of extinction coefficient (k) when increasing the value of doping this may be due to increasing the absorption coefficient [38, 39].

The refractive index (n) was considered at different wavelengths based on optical reflectivity (R) by using the relation (7) [41, 42]:

$$n = \frac{1 + R^{\frac{1}{2}}}{1 - R^{\frac{1}{2}}} \quad (7)$$

The behaviors n via wavelength of CdSe: 2 and 4 % silver films is shown in Figure (8), We can see from this figure that the value of (n) increases with increasing silver concentration due to the increases in compactness of films after doping simultaneously with the increasing of the crystallite size [43, 44].

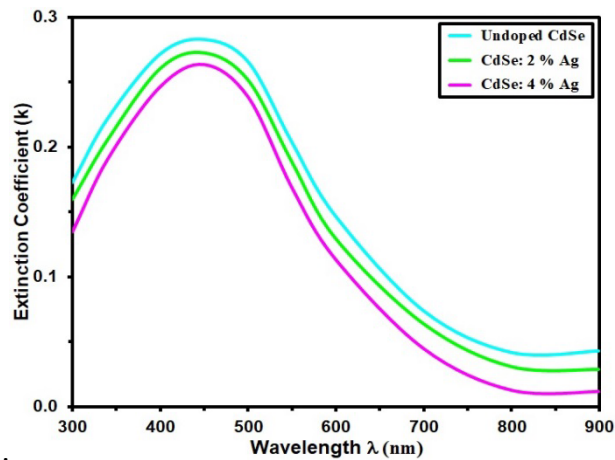


Fig. 7. Extinction coefficient of pure & CdSe:Ag films with different dopants.

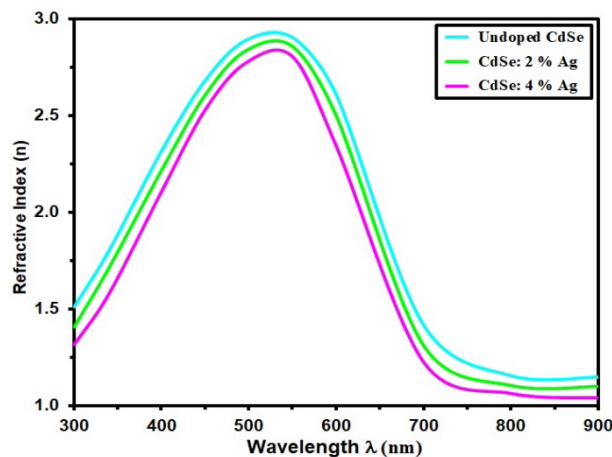


Fig. 8. Refractive index of pure & CdSe:Ag films with different dopants.

4. Conclusion

Silver doping affects the structural, optical properties and Surface topography of CdSe and Ag-doped CdSe at 2 % and 4 % doping thin films. As silver was added to CdSe thin films, the hexagonal structure did not change. D , microstrain and dislocation density were obtained via Ag content. CdSe, CdSe: Ag 2 and 4 % thin films reveal that the surface is nanostructured with

particle sizes ranging from 71-54 nm, respectively. At 300-900 nm wavelengths, transmittance spectra were measured. Due to Ag-doping, E_g was reduced (from 1.85 eV to 1.75 eV).

Acknowledgments

The authors appreciate Mustansiriya University (uomustansiriya.edu.iq) and Alnukhba University College for their support.

References

- [1] M. S. Kang, A. Sahu, D. J. Norris, C. D. Frisbie, *Nano Lett.* 10, 3727 (2010); <https://doi.org/10.1021/nl102356x>
- [2] S. K. Tripathi, *J. Mater. Sci.* 45, 5468 (2010); <https://doi.org/10.1007/s10853-010-4601-6>
- [3] K. Sharma, A. S. Al-Kabbi, G. S. Saini, S. K. Tripathi, *Materials Research Bulletin* 47, 1400 (2012); <https://doi.org/10.1016/j.materresbull.2012.03.008>
- [4] E. El-Menyawy, A. A. Azab, *Optik*, 168, 217 (2018); <https://doi.org/10.1016/j.ijleo.2018.04.056>
- [5] S. Mathuri, K. Ramamurthi, R. R. Babu, *Thin Solid Film* 625, 138 (2017); <https://doi.org/10.1016/j.tsf.2017.01.053>
- [6] R. Sahebi, M. R. Roknabadi, M. Behdani, *Optik* 204, 164204 (2020); <https://doi.org/10.1016/j.ijleo.2020.164204>
- [7] K. Girija, S. Thirumalairajan, S. M. Mohan, J. Chandrasekaran, *Chalcogenide Letters* 6(8), 351 (2009);
- [8] Y. M. Niquet, G. Allan, C. Deleue, M. Lannoo, *Appl. Phys. Lett.* 77, 1182 (2000); <https://doi.org/10.1063/1.1289659>
- [9] A. L. Efros, M. R. Annu, *Rev. Mater. Sci.* 30, 475 (2000); <https://doi.org/10.1146/annurev.matsci.30.1.475>
- [10] T. C. Santhosh., K. V. Bangera, G. K. Shivakumar, *Mater. Sci. Semicond. Process.* 68, 114 (2017); <https://doi.org/10.1016/j.mssp.2017.06.004>
- [11] R. Sahebi, M. R. Roknabadi, M. Behdani, *Mater. Res. Express* 6, 126453 (2019); <https://doi.org/10.1088/2053-1591/ab6c17>
- [12] M. A. Hernandez-Perez, J. Aguilar-Hernandez, G. Contreras-Puente, J. R. Vargas-Garcia, E. Rangel-Salinas, *Physica E* 40, 2535 (2008); <https://doi.org/10.1016/j.physe.2007.10.102>
- [13] K. Sharma, A. S. Al-Kabbi, G. S. Saini, S. K. Tripathi, *Materials Research Bulletin* 47, 1400 (2012); <https://doi.org/10.1016/j.materresbull.2012.03.008>
- [14] E. S. Hassan, A. K. Elttayef, S. H. Mostafa, M. H. Salim, S. S. Chiad, *Journal of Materials Science: Materials in Electronics*, 30 (17), 15943-15951, (2019); <https://doi.org/10.1007/s10854-019-01954-1>
- [15] P. P. Hankare, V. M. Bhuse, K. M. Garadkar, S. D. Delekar, I. S. Mulla, *Semicond. Sci. Technol.* 19, 70 (2004); <https://doi.org/10.1088/0268-1242/19/1/012>
- [16] A. A. Yadav, M. A. Barote, E. U. Masumdar, *Mater. Chem. Phys.* 121, 53 (2010); <https://doi.org/10.1016/j.matchemphys.2009.12.039>
- [17] S. Thanikaikarasan, T. Mahalingam, M. Raja, Taekyu Kim, Yong Deak Kim, *J. Mater. Sci. Mater. Electron* 20, 727 (2009); <https://doi.org/10.1007/s10854-008-9794-y>
- [18] B. Singh, J. Singh, R. Kaur, R. K. Moudgil, S. K. Tripathi, *RSC Adv.* 7, 53951 (2017); <https://doi.org/10.1039/C7RA02904G>
- [19] N. Y. Jamil, M. T. Mahmood, N. A. Mustafa, *Rafidain Journal of Science*, 23 (1) 116 (2012); <https://doi.org/10.33899/rjs.2012.29447>
- [20] M. D. Sakhil, Z. M. Shaban, K. S. Sharba, N. F. Habub, K. H. Abass, S. S. Chiad, A. S. Alkelaby, *NeuroQuantology*, 18 (5), 56 (2020);

<https://doi.org/10.14704/nq.2020.18.5.NQ20168>

- [21] A. J. Ghazai, O. M. Abdulmunem, K. Y. Qader, S. S. Chiad, N. F. Habubi, AIP Conference Proceedings 2213 (1), 020101 (2020); <https://doi.org/10.1063/5.0000158>
- [22] M. R. Bhuiyan, M. A. Azad, S. M. Hasan, Indian Journal of pure and Applied Physics, 49, 180 (2011); <https://doi.org/10.1016/j.clema.2021.100030>
- [23] E. H. Hadi, D. A. Sabur, S. S. Chiad, N. F. Habubi, K. H. Abass, Journal of Green Engineering, 10 (10), 8390 (2020); <https://doi.org/10.1063/5.0095169>
- [24] H. A. Hussin, R. S. Al-Hasnawy, R. I. Jasim, N. F. Habubi, S. S. Chiad, Journal of Green Engineering, 10(9), 7018 (2020); <https://doi.org/10.1088/1742-6596/1999/1/012063>
- [25] D. M. A. Latif, S. S. Chiad, M. S. Erhayief, K. H. Abass, N. F. Habubi, H. A. Hussin, Journal of Physics, Conference Series 1003(1), 012108 (2018); <https://doi.org/10.1088/1742-6596/1003/1/012108>
- [26] F. Haque, K. S. Rahman, Akhtaruzzaman, H. Abdullah, T. S. Kiong, N. Amin, S. K. Tiong, Mater. Res. Express 5, 096409 (2018); <https://doi.org/10.1088/2053-1591/aad6c6>
- [27] K. Punitha, R. Sivakumar, C. Sanjeeviraja, V. Sathe, V. Ganesan, J. Appl. Phys. 116, 213502 (2014); <https://doi.org/10.1063/1.4903320>
- [28] K. Punitha, R. Sivakumar, C. Sanjeeviraja, V. Sathe, V. Ganesan, Appl. Surf. Sci. 344, 89 (2015); <https://doi.org/10.1016/j.apsusc.2015.03.095>
- [29] M. S. Othman, K. A. Mishjil, H. G. Rashid, S. S. Chiad, N. F. Habubi, I. A. Al-Baidhany, Journal of Materials Science: Materials in Electronics, 31(11), 9037 (2020); <https://doi.org/10.1007/s10854-020-03437-0>
- [30] R. S. Ali, H. S. Rasheed, N. F. Habubi, S. S. Chiad, Letters, 20(1), 63 (2023); <https://doi.org/10.15251/CL.2023.201.63>
- [31] H. T. Tung, D. V. Thuan, J. H. Kiat, D. H. Phuc, Appl. Phys. A 125, 505 (2019); <https://doi.org/10.1007/s00339-019-2797-0>
- [32] E. S. Hassan, A. K. Elttayef, S. H. Mostafa, M. H. Salim and S. S. Chiad. Journal of Materials Science: Materials in Electronics, 30 (17), 15943 (2019); <https://doi.org/10.1155/2014/684317>
- [33] H. T. Salloom, E. H. Hadi, N. F. Habubi, S. S. Chiad, M. Jadan, J. S. Addasi, Digest Journal of Nanomaterials and Biostructures, 15 (4), 189 (2020); <https://doi.org/10.15251/DJNB.2020.154.1189>
- [34] K. Saritha, S. Rasool, K. R. Reddy, M. Tivanov, A. Saad, A. Trofimova, V. Gremenok, Mater. Res. Express 6, 106439 (2019); <https://doi.org/10.1088/2053-1591/ab4078>
- [35] R. S. Ali, M. K. Mohammed, A. A. Khadayeir, Z. M. Abood, N. F. Habubi and S. S. Chiad, Journal of Physics: Conference Series, 1664 (1), 012016 (2020); <https://doi.org/10.1088/1742-6596/1664/1/012016>
- [36] S. S. Chiad, H. A. Noor, O. M. Abdulmunem, N. F. Habubi, M. Jadan, J. S. Addasi, Journal of Ovonic Research, 16 (1), 35 (2020).
- [37] N. N. Jandow, M. S. Othman, N. F. Habubi, S. S. Chiad, K. A. Mishjil, I. A. Al-Baidhany, Materials Research Express, 6 (11), 116434 (2020); <https://doi.org/10.1088/2053-1591/ab4af8>
- [38] V. S. Raut, C. D. Lokhande, V. V. Killedar, J. Mater. Sci., Mater. Electron. 28, 3140 (2017); <https://doi.org/10.1007/s10854-016-5902-6>
- [39] E. S. Hassan, K. Y. Qader, E. H. Hadi, S. S. Chiad, N. F. Habubi, K. H. Abass, Nano Biomedicine and Engineering, 12(3), 205 (2020); <https://doi.org/10.5101/nbe.v12i3.p205-213>
- [40] R. S. Ali, N. A. H. Al Aaraji, E. H. Hadi, N. F. Habubi, S. S. Chiad, Journal of Nanostructures, 10(4), 810 (2020); <https://doi.org/10.22052/jns.2020.04.014>
- [41] S. S. Chiad, A. S. Alkelaby, K. S. Sharba, Journal of Global Pharma Technology, 11(7), 662 (2020); <https://doi.org/10.14704/nq.2020.18.5.NQ20168>
- [42] N. Y. Ahmed, B. A. Bader, M. Y. Slewa, N. F. Habubi, S. S. Chiad, NeuroQuantology, 18(6), 55 (2020); <https://doi.org/10.14704/nq.2020.18.6.NQ20183>

- [43] A. A. Khadayeir, R. I. Jasim, S. H. Jumaah, N. F. Habubi, S. S. Chiad, Journal of Physics: Conference Series, 1664, 012009 (2020); <https://doi.org/10.1088/1742-6596/1664/1/012009>
- [44] Mohamed Hassen, Rim Riahi, Fakher Laatar, Hatem Ezzaouia, Surfaces and Interfaces, 18, 100408 (2020); <https://doi.org/10.1016/j.surfin.2019.100408>